PYROLYSIS OF PINE AND BEECH WOOD SAMPLES UNDER ISOTHERMAL EXPERIMENTAL CONDITIONS. THE DETERMINATION OF KINETIC TRIPLETS

BOJAN Ž. JANKOVIĆ[*] and MARIJA M. JANKOVIĆ[**]

[*]*Faculty of Physical Chemistry, Department for Dynamics and Matter Structure, University of Belgrade, Studentski trg 12-16, P. O. Box 137, 11001 Belgrade, Serbia*
[**]*Radiation and Environmental Protection Department, University of Belgrade, Institute Vinča, P.O. Box 522, 11001 Belgrade, Serbia*

Received January 9, 2013

The pyrolysis process of pine and beech wood samples was investigated by the isothermal thermogravimetric technique, at five different operating temperatures, in nitrogen flowing stream. It was found that the isothermal pyrolysis process of wood samples can be described by the three-dimensional diffusion mechanisms, with different reaction geometry (Jander's type for pine, and Ginstling-Brounstein's type for beech). The evaluated models for both processes represent the global one-step reaction mechanisms. Some differences in the values of the kinetic parameters and diffusion geometry of the volatile products were established, probably resulting from sensitive alterations of the structure and the chemical composition of the investigated wood samples, occurring during the pyrolysis process.

Keywords: wood, pyrolysis, kinetics, diffusion mechanism, apparent activation energy

INTRODUCTION

Wood and the other forms of biomass are some of the main renewable solid energy resources available and provide the source of liquid, gaseous and solid fuels. Biomass potential includes wood, animal and plant wastes. Biomass is the only organic petroleum substitute that is renewable. The term "biomass" refers to forestry, purpose-grown agricultural crops, trees and plants, and organic, agricultural, agro-industrial, and domestic wastes (municipal and solid waste). Biomass is the name given to the plant matter that is created by photosynthesis, in which the sun's energy converts water and CO_2 into organic matter. Thus biomass is directly or indirectly the result of plant growth, including wood plantations, agricultural residues, forestry residues, animal wastes, etc.[1]

The thermochemical biomass conversion does include a number of possible routes to produce useful fuels and chemicals from the initial biomass feedstock. The basis of thermochemical conversion is the pyrolysis process, which includes all chemical changes occuring when heat is applied to a material in the absence of oxygen. The products of biomass pyrolysis include water, charcoal (or more exactly a carbonaceous solid), oils or tars, and gases comprising methane, hydrogen, carbon monoxide, and carbon dioxide. The nature of the changes in pyrolysis depends on the material being pyrolyzed, the final temperature of the pyrolysis process and the rate at which it is heated up.[2] As typical lignocellulosic biomass materials, such as wood, straws and stalks, are poor heat conductors, the management of the heating rate requires that the size of the particles being heated be quite small.[3-6] Depending on the thermal environment and the final temperature, pyrolysis will yield mainly char at low temperatures, less than 450 °C, when the heating rate is quite slow, and mainly gases at high temperatures, greater than 800 °C, with rapid heating rates.[7,8] At an intermediate temperature and under relatively high heating rates, the main product is a liquid bio-oil, a relatively recent discovery, which is being turned to commercial applications. The pyrolysis of complex materials

like wood and lignocellulosic biomass can be studied by focusing the attention on gaseous and condensable products or by following the solid weight loss. This second method has been more widely applied and is a useful practical approach when the main interest lies in the solid product, as in charring, high temperature carbonization and activation. In these cases, the use of thermal methods (such as the thermogravimetric analysis (TGA) or differential thermal analysis (DTA)) allows kinetic studies to be carried out by a simple and rapid experimental procedure. Nevertheless, a wide diversity of results have been reported in the literature.[9-11] In spite of the numerous experimental studies existing on biomass pyrolysis and kinetic modelling, there is no generally accepted model that can predict the pyrolysis rate and provide *a priori* information about final conversion over a wide range of particle sizes for a particular species of biomass.[12-23]

The objective of this study is to investigate the kinetics of the pyrolysis process of two types of wood (pine and beech), conducted by the thermogravimetric analysis (TGA) under isothermal experimental conditions, at different operating temperatures (280, 290, 300, 310 and 320 °C). For both wood types considered, the kinetic analysis and mechanistic interpretation of the process are presented. The results of kinetic modeling of wood pyrolysis obtained under isothermal conditions are important and necessary for the development of fast pyrolysis technologies, and in some cases, for the devolatilization stage of gasifiers and combustors.[16]

This work represents a comprehensive study of the isothermal wood pyrolysis, where the considered research is related to the classical kinetic approach from the point of view of solid-state reaction mechanisms.

EXPERIMENTAL

Thermo-analytical measurements were carried out on the wood samples derived from pine (*Pinus sylvestris L.*) and beech (*Fagus moesiaca*). Experimental samples were prepared from the wood, which was air conditioned at the temperature of $T = 20$ °C, and kept at the relative humidity of 60%. The considered wood material was comminuted to particles ranging from 0.52 to 1.52 mm, in order to minimize the effect of heat conduction during the thermal decomposition process.[24,25]

The isothermal investigations were carried out on a thermogravimetric analyzer (TA Instruments SDT 2960 device capable of simultaneous TGA-DTA measurements), using sample portions with $m \approx 20$ mg. Sample mass losses were recorded on TG curves during isothermal mesurements and the experiments were carried out at five different operating temperatures (280, 290, 300, 310 and 320 °C). For all samples, the value of the heating rate used to achieve the desired operating temperature was $\beta = 100$ °C min^{-1}. All the isothermal experiments were carried out in the atmosphere of flowing nitrogen (the flowing rate of $\varphi = 50$ mL min^{-1}), with the sample placed in an open platinum crucible.

Theory

The rate of a solid-state decomposition process can be generally described by the equation:

$$\frac{d\alpha}{dt} = kf(\alpha) \tag{1}$$

where k is the rate constant ($k = A \cdot \exp(-E_a/RT)$, (where A is the pre-exponential (frequency) factor, E_a is the apparent activation energy, T is the absolute temperature and R is the gas constant), $f(\alpha)$ is the differential reaction model and α is the conversion fraction or the extent of reaction ($\alpha = (m_o - m_T)/(m_o - m_f)$, m_o, m_T and m_f are the initial, actual and final mass of the sample in the TGA curves, respectively). Integrating the above equation gives the integral rate law in the form:[26]

$$g(\alpha) = kt \tag{2}$$

where $g(\alpha)$ is the integral reaction model. The function $g(\alpha)$ is dependent on the mechanism of the reaction, and this dependence is often used to infer an atomic reaction mechanism. Substituting the Arrhenius equation in Eq. (2), we can obtain Eq. (3):

$$g(\alpha) = A\exp\left(-\frac{E_a}{RT}\right)t \tag{3}$$

Isoconversional method

Isoconversional (or "model-free") methods calculate the apparent activation energy (E_a) without modelistic assumptions, which is usually done by grouping terms such as the pre-exponential factor (A) and reaction model into the intercept of a linear equation and using the slope of that equation to calculate the apparent activation energy. The pre-exponential factor (A) can be calculated from the intercept of the linear equation, but requires modelistic assumptions for such a determination. Therefore, model-free methods usually report only apparent activation energies. It can be mentioned that the terms "model-free" and isoconversional are sometimes used interchangeably, however, not all model-free methods are isoconversional (for example, the Kissinger method is one of these exceptions because it does not calculate E_a values at progressive α values, but assumes a constant apparent activation energy). Isoconversional approaches can be used to analyze both isothermal (where the temperature changes) and nonisothermal

(where the heating rate changes) data. The standard isoconversional method[27] is based on taking the natural logarithm of Eq. (3) giving:

$$-\ln(t_{\alpha,i}) = \ln\left[\frac{A_\alpha}{g(\alpha)}\right] - \frac{E_{a,\alpha}}{RT_i} \quad (4)$$

where $t_{\alpha,i}$ is the time at a given value of α (α = const.) for operating temperature T_i, while A_α represents the pre-exponential factor at a given value of conversion, α. From different isothermal runs for which the same values of α were reached, the plots $-\ln(t_{\alpha,i})$ versus $1/T_i$ with a slope proportional to E_a can be drawn. The corresponding plots may show a curvature, which may indicate the existence of a complex multi-step mechanism or a change in the rate-determining step, which is directly reflected in the trend of curve $E_{a,\alpha} = E_{a,\alpha}(\alpha)$.

Model-fitting methods

Eq. (2) can be used for calculation of the rate constant (k), after introducing the various expressions for $g(\alpha)$. The rate equations can be divided into three general groups: a) phase-boundary and first-order reactions, b) the diffusion controlled reactions, and c) reactions described by the Avrami equation.[28] The plot of the left side of Eq. (2) against time would lead to a straight line whose slope gives the rate constant, k. By the introduction of k in the linear form of the Arrhenius equation ($\ln k = \ln A - E_a/RT_i$), the values of kinetic parameters ($\ln A$, E_a) can be calculated. In order to separate the actual reaction kinetics from the analysis of a single isothermal, both the method of "reduced time" master plots,[29] which represents α versus $t/t_{0.50}$ ($t_{0.50}$ is the time for α = 0.50) and the "ln-ln" method, which requires determination of the slope m (parameter m) of the plot of ln[-ln(1-α)] versus ln$t$, were used. The values of m reported by Hancock and Sharp[30] for the different kinetic models are included in Table 1.

If m is below unity, the reaction is in favor of diffusion processes, whereas if m is located between unity and two ($1<m<2$), the phase boundary controlled process is possibly dominant. If a single reaction mechanism operates through the temperature range and several data sets are isokinetic, they will plot as a set of parallel lines with a constant value of m.[31]

RESULTS AND DISCUSSION

Isothermal mass loss experiments for pine and beech wood

Fig. 1 shows the isothermal mass loss experiments performed at different operating temperatures (280, 290, 300, 310 and 320 °C), for the pyrolysis process of pine (colored curves) and beech (black curves) wood samples, respectively.

Table 1
Algebraic expressions of $g(\alpha)$ functions and theoretical slopes of the plots of ln[-ln(1-α)] against ln$t$

Mechanism	Function of reaction mechanism	Kinetic parameter
Phase boundary reaction	$g(\alpha)$	m
R1, F0	α	1.24
R2	$1-(1-\alpha)^{1/2}$	1.11
R3	$1-(1-\alpha)^{1/3}$	1.07
Mechanism	Function of reaction mechanism	Kinetic parameter
Random nucleation, Avrami	$g(\alpha)$	m
A1, F1	$-\ln(1-\alpha)$	1.00
A2	$[-\ln(1-\alpha)]^{1/2}$	2.00
A3	$[-\ln(1-\alpha)]^{1/3}$	3.00
Mechanism	Function of reaction mechanism	Kinetic parameter
Diffusion mechanism	$g(\alpha)$	m
D1	α^2	0.62
D2	$(1-\alpha)\ln(1-\alpha)+\alpha$	0.57
D3	$[1-(1-\alpha)^{1/3}]^2$	0.54
D4	$1-2\alpha/3-(1-\alpha)^{2/3}$	0.55

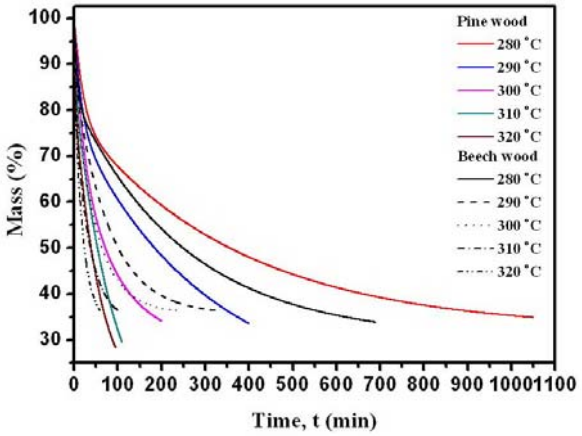

Figure 1: Isothermal thermogravimetric (TG) curves for pyrolysis process of pine (colored curves) and beech (black curves) wood samples, collected from 280 °C to 320 °C (Color reproduction in online version)

Isothermal mass loss experiments (280-320 °C) for the pyrolysis process of pine wood (Fig. 1 – colored TG curves) show a rapid mass loss in the first 50 minutes of heating, followed by a period of slower mass loss. It should be noted that below the temperature of 200 °C (during the process of raising the temperature to the desired operating temperature), we can expect that only non-combustible gases, primarily water vapor, with traces of carbon dioxide, formic and acetic acids, and glyoxal, are produced. The dehydration of the sorbed water is complete. After reaching the operating temperature of 280 °C, we now probably have the same above-mentioned gases, but with a greatly reduced quantity of water vapor, and some carbon monoxide. In this case, the reactions are characterized by an endothermic effect. At operating temperatures higher than 280 °C (namely, in the experimentally observed range of selected operating temperatures), active pyrolysis takes place under exothermic conditions. The rate of mass loss decreased gradually with time until the point when wood was transformed into stable charcoal with a constant final mass. It should be noted that with an increase of operating temperature, the slope of isothermal TG curves increases, with the curve shifted to the region with lower reaction times. The lowest temperature runs (280 °C) show the smallest mass loss at the end of the long experiment. It seems that, up to an operating temperature of 320 °C, the residual mass loss (m_f (or m_∞)) decreases with the increase in operating temperature.

The isothermal experiments (280-320 °C) for the pyrolysis process of beech wood (Fig. 1 – black TG curves) show a rapid mass loss in the first 20 minutes of heating, followed by a period of slower mass loss. Similar observations can be made in this case, as those on the thermal behavior of pine wood (see above). It should be noted that the slopes of the isothermal TG curves for the pyrolysis of beech wood are slightly different, compared to the slopes of the isothermal TG curves for pine wood pyrolysis. Also, the duration of the pyrolytic process of beech wood is shorter than the duration of the pyrolytic process of pine wood (for example, if we compare the time scale at the operating temperature of 280 °C). Similarly to the pyrolysis process of pine wood, with an increase of operating temperature, the slope of the isothermal TG curves increases, with the curve shifted to the region with lower reaction times (Fig. 1). This behavior is characteristic of all the reaction systems that are thermally activated. In addition, the lowest temperature runs (280 °C) showed the smallest mass loss at the end of the experiment. However, at the other operating temperatures (T > 280 °C), slight variations in the final mass change were observed. These small variations of final mass are dependent on the amount of sample and the manner of packing of the sample into the platinum crucible.[32]

Isoconversional (model-free) analysis

Figs. 2 and 3 show the isoconversional plots of $-\ln t$ versus $1/T$ (Eq. (4)), for pine and beech wood isothermal pyrolysis processes, respectively, at different and constant values of the conversion fraction. The plots were obtained in a wide range of α values (α = 0.05-0.95, in steps of 0.05).

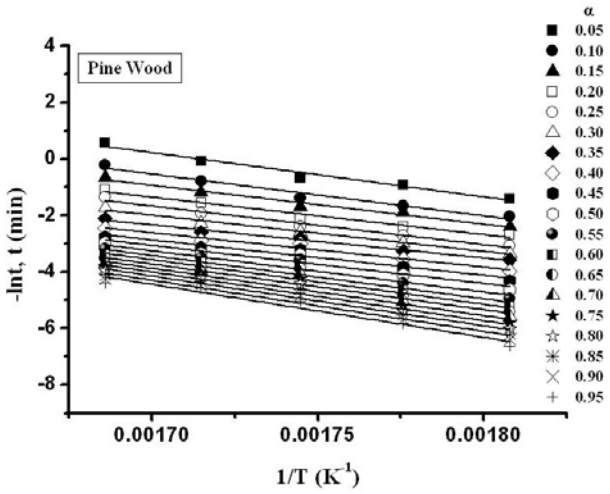

Figure 2: Isoconversional plots of –ln*t* versus 1/*T* (Eq. (4)), for pine wood isothermal pyrolysis, at different and constant values of conversion fraction (α = 0.05-0.95, in steps of 0.05)

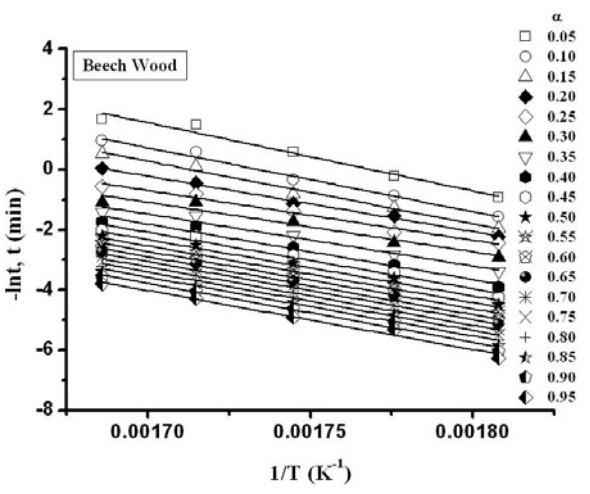

Figure 3: Isoconversional plots of –ln*t* versus 1/*T* (Eq. (4)), for beech wood isothermal pyrolysis, at different and constant values of conversion fraction (α = 0.05-0.95, in steps of 0.05)

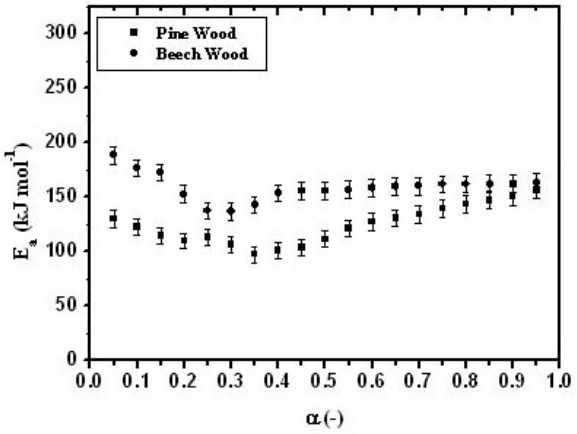

Figure 4: Dependence of apparent activation energy (E_a) on conversion fraction (α), obtained by isothermal isoconversional ("model-free") analysis, for pine and beech wood pyrolysis processes

The plots do not show abrupt curvatures at any α value, but only a small variation in the slope, which does not make them perfectly parallel for each α, in the case of both observed systems (Figs. 2 and 3).

Fig. 4 shows the results of isoconversional analysis for the pyrolysis process of pine and beech wood samples.

The dependences of the apparent activation energy (E_a) on the extent of reaction (α) for both considered wood samples are similar, but not identical. Namely, in the case of pine wood pyrolysis, we can see that there is some variation of E_a value with α (Fig. 4; symbol ■), but this variation is not dramatically large. If we look closely at the dependence of $E_a = E_a(\alpha)$ for pine wood pyrolysis, we can see that there are three regions with a change of E_a on α: the first region ($0.05 \leq \alpha \leq 0.25$), where there is a gradual decrease in the value of E_a (from 130 kJ mol^{-1} to approximately 113.6 kJ mol^{-1}); the second region ($0.25 \leq \alpha \leq 0.35$), where there is also a downward trend in E_a with α, from the 113.6 kJ mol^{-1} to 97.5 kJ mol^{-1}; and the third region ($0.40 \leq \alpha \leq 0.95$), where there is a gradual increase of E_a value with α (from 101.1 kJ mol^{-1} to approximately 157.4 kJ mol^{-1}). However, in the range of α values, from α = 0.60 to α = 0.90, there is a slight increase in E_a values so that the variations of E_a values with respect to their amplitudes are quite small. This conclusion is made on a rational basis, taking into account that the change in E_a values in the considered α range is within ±10% of the average value (the average value is equal to 139.3 kJ mol^{-}

[1]; in our current case, the error is even below ± 10%) (This error is quite acceptable, given the experimental technique based on which the data were obtained for the calculation of E_a, which of course, includes the error arising from the use of Eq. (4)). In that case, we can assume that in the observed conversion region, the value of E_a is approximately constant ($<E_a>$ = 139.3 kJ mol^{-1}). The value of $<E_a>^{pine}$ = 139.3 kJ mol^{-1} is primarily responsible for cellulose degradation.[16,33] Generally, at temperatures above 100 °C, chemical bonds begin to break. The rate at which the bonds are broken increases as the temperature increases. Between 100 °C and 200 °C, products, such as carbon dioxide, traces of organic compounds and water vapor, are produced. Above 200 °C, lignin and cellulose break down, producing tars and flammable volatiles that can diffuse into the surrounding environment.[34] The obtained value of the apparent activation energy for the pine wood pyrolysis (Fig. 4), in the conversion range where E_a does not show significant variation with α (139.3 kJ mol^{-1}), enters the range of E_a values for wood pyrolysis in nitrogen (from 63.0 kJ mol^{-1} to 140.0 kJ mol^{-1}), for temperatures less than 320 °C.[35] The value of 139.3 kJ mol^{-1} for pine wood pyrolysis represents the averaged value, since for $\alpha > 0.40$ there is a gradual increase in E_a, which may include the process involving consecutive and parallel decomposition reactions. We can expect that the hemicelluloses start to decompose before cellulose at lower operating temperatures, whereas cellulose starts to decompose at higher operating temperatures (above 300 °C).[36] This can be explained by the lower thermal stability of hemicelluloses than that of cellulose, presumably due to their lack of crystallinity. Followed by the decomposition of cellulose, the main decomposition of lignin at high operating temperatures is presented. This is important to note because the lignin decomposition process can be studied by means of specific lignin ion fragments.

In the case of beech wood pyrolysis, we can see that there is some variation of E_a value with α, as in pine wood pyrolysis (Fig. 4; symbol ●), but the observed variation is not dramatically large. Also, we can see that there are three regions in the variation of E_a with α: the first region ($0.05 \leq \alpha \leq 0.25$) characterized by the decrease of E_a value with α (from 188.8 kJ mol^{-1} to 137.6 kJ mol^{-1}); the second region ($0.30 \leq \alpha \leq 0.40$), where we have the opposite behavior in relation to pine wood pyrolysis, so an increase in E_a value with α appears (from 136.9 kJ mol^{-1} to 153.4 kJ mol^{-1}); and the third region ($0.40 \leq \alpha \leq 0.95$), where the value of E_a is approximately constant and this value is $<E_a>^{beech}$ = 159.4 kJ mol^{-1} (similarly as in the case of pine wood pyrolysis, the change in E_a values in α range of $0.40 \leq \alpha \leq 0.95$ is within ±10% of the average value) (Fig. 4). In general, the values of E_a for beech wood pyrolysis are higher than the values of E_a for the pyrolysis of pine wood. The differences in the values of E_a for the investigated wood samples may arise from different percentage of wood constituents.[37]

From the isoconversional analysis, for both wood samples, we can conclude that in the considered range of operating temperatures, the hemicelluloses decomposition occurred with lignin transformation, which probably appeared as a result of a condensation reaction. In addition, the maximum rate of mass loss occurred, the hemicelluloses decomposition continued, and cellulose decomposition was evident.

It can be pointed out that on the basis of the used experimental range of operating temperatures, the thermal degradation of pine and beech wood represents the combined approach of probably two pathways, i.e., the low-temperature and the high-temperature pathways, one occurring at high temperatures (T > 300 °C) (including combustible gases, CO_2, H_2O, char residue), and the other at lower temperatures (including noncombustible gases, CO, CO_2, H_2O, char residue). It should be noted that the thermal decomposition can also take place through the so-called "char forming" pathway (over 250 °C). In this process, cellulose is first transformed (with a slightly endothermic effect) to unstable, "active" cellulose, which further decomposes so that reaction products are mainly carbon dioxide and water, and the "backbone" of cellulose containing a lot of carbon.[38]

Model-fitting analysis

Taking into account the average values of E_a for both investigated pyrolysis processes, it is possible to describe the whole reaction interval by a single kinetic model, even if the real mechanism is complex. Taking into account the conversion intervals, which are noted above, for each of the investigated wood systems, the model-fitting method based on Eq. (2) was applied.

The values of the rate constant (k) and the results obtained from the statistical analysis of the experimental data (Adj.R-Square (R^2) and

Residual sum of squares (RSS)) using Eq. (2), for the isothermal pyrolysis of pine wood ($0.60 \leq \alpha \leq 0.90$) are listed in Table 2.

For the pyrolysis of pine wood (Table 2), the model-fitting method described by Eq. (2) demonstrated the presence of several statistically equivalent reaction models with different values of k, at each of the considered operating temperatures (R3, A2, D2, D3 and D4 models at 280 °C, R2, R3, A3, D2 and D4 models at 290 °C, R3, D3 and D4 models at 300 °C, R2, A3 and D1 models at 310 °C, R2, R3, A2, A3, D2 and D4 models at 320 °C).

The values of the rate constant (k) and the results obtained from the statistical analysis of the experimental data (Adj.R-Square (R^2) and Residual sum of squares (RSS)) using Eq. (2), for the isothermal pyrolysis of beech wood ($0.40 \leq \alpha \leq 0.95$) are listed in Table 3.

Table 2
Numerical data calculated from isothermal analysis (Eq. (2)) for the pyrolysis of pine wood in α range $0.60 \leq \alpha \leq 0.90$

T = 280 °C			
Mechanism	$k(T)$ (min^{-1})	R^2	*RSS*
R1, F0	6.99810×10^{-4}	0.97845	0.00630
R2	7.46820×10^{-4}	0.99651	0.00114
R3	6.44387×10^{-4}	0.99915	2.05494×10^{-4}
A1, F1	0.00326	0.99898	0.00635
A2	0.00131	0.99917	8.42745×10^{-4}
A3	8.17589×10^{-4}	0.99762	9.33403×10^{-4}
D1	0.00107	0.99067	0.00631
D2	0.00104	0.99900	6.39059×10^{-4}
D3	5.17386×10^{-4}	0.99636	5.71471×10^{-4}
D4	3.04848×10^{-4}	0.99997	1.87427×10^{-6}
T = 290 °C			
Mechanism	$k(T)$ (min^{-1})	R^2	*RSS*
R1, F0	0.00156	0.99283	0.00244
R2	0.00165	0.99997	1.23305×10^{-5}
R3	0.00141	0.99895	2.91417×10^{-4}
A1, F1	0.00710	0.99150	0.05962
A2	0.00289	0.99884	0.00133
A3	0.00180	0.99972	1.27371×10^{-4}
D1	0.00238	0.99884	9.02991×10^{-4}
D2	0.00230	0.99903	7.10035×10^{-4}
D3	0.00112	0.98533	0.00258
D4	6.66461×10^{-4}	0.99607	2.42095×10^{-4}
T = 300 °C			
Mechanism	$k(T)$ (min^{-1})	R^2	*RSS*
R1, F0	0.00353	0.97376	0.00710
R2	0.00379	0.99437	0.00173
R3	0.00328	0.99791	4.77627×10^{-4}
A1, F1	0.01668	0.99960	0.00238
A2	0.00669	0.99791	0.00198
A3	0.00415	0.99577	0.00155
D1	0.00542	0.98740	0.00796
D2	0.00532	0.99777	0.00134
D3	0.00265	0.99808	2.86864×10^{-4}
D4	0.00156	0.99976	1.24634×10^{-5}
T = 310 °C			
Mechanism	$k(T)$ (min^{-1})	R^2	*RSS*
R1, F0	0.00636	0.99538	0.00139
R2	0.00665	0.99965	1.14092×10^{-4}
R3	0.00569	0.99773	5.48125×10^{-4}
A1, F1	0.02842	0.98860	0.06921

A2	0.01161	0.99766	0.00235
A3	0.00726	0.99913	3.40705×10^{-4}
D1	0.00962	0.99970	2.05302×10^{-4}
D2	0.00924	0.99775	0.00143
D3	0.00447	0.98142	0.00282
D4	0.00268	0.99382	3.30795×10^{-4}
	T = 320 °C		
Mechanism	$k(T)$ (min^{-1})	R^2	*RSS*
R1, F0	0.00723	0.99106	0.00281
R2	0.00760	0.99991	2.92239×10^{-5}
R3	0.00652	0.99950	1.27759×10^{-4}
A1, F1	0.03268	0.99329	0.04295
A2	0.01330	0.99942	6.14503×10^{-4}
A3	0.00830	0.99987	5.20787×10^{-5}
D1	0.01097	0.99810	0.00137
D2	0.01058	0.99953	3.14716×10^{-4}
D3	0.00515	0.98762	0.00198
D4	0.00307	0.99719	1.58120×10^{-4}

Table 3
Numerical data calculated from isothermal analysis (Eq. (2)) for the pyrolysis of beech wood in α range $0.40 \leq \alpha \leq 0.95$

	T = 280 °C		
Mechanism	$k(T)$ (min^{-1})	R^2	*RSS*
R1, F0	0.00111	0.94610	0.08794
R2	0.00115	0.99230	0.01283
R3	9.91262×10^{-4}	0.99867	0.00164
A1, F1	0.00510	0.99449	0.18090
A2	0.00207	0.99802	0.01065
A3	0.00130	0.99357	0.01363
D1	0.00160	0.98044	0.06400
D2	0.00154	0.99853	0.00437
D3	7.89502×10^{-4}	0.98550	0.01149
D4	4.52908×10^{-4}	0.99931	1.77412×10^{-4}
	T = 290 °C		
Mechanism	$k(T)$ (min^{-1})	R^2	*RSS*
R1, F0	0.00287	0.92040	0.10204
R2	0.00303	0.98103	0.02537
R3	0.00263	0.99269	0.00729
A1, F1	0.01375	0.99948	0.01413
A2	0.00550	0.99239	0.03316
A3	0.00343	0.98439	0.02665
D1	0.00418	0.96285	0.09648
D2	0.00409	0.99185	0.01964
D3	0.00214	0.99517	0.00317
D4	0.00121	0.99832	3.51705×10^{-4}
	T = 300 °C		
Mechanism	$k(T)$ (min^{-1})	R^2	*RSS*
R1, F0	0.00412	0.91630	0.09088
R2	0.00441	0.97872	0.02484
R3	0.00385	0.99117	0.00777
A1, F1	0.02032	0.99983	0.00424
A2	0.00804	0.99136	0.03310
A3	0.00499	0.98322	0.02498
D1	0.00606	0.95839	0.09376
D2	0.00599	0.98954	0.02228
D3	0.00318	0.99670	0.00196

D4	0.00178	0.99731	5.02722×10^{-4}
	T = 310 °C		
Mechanism	$k(T)$ (min^{-1})	R^2	*RSS*
R1, F0	0.00786	0.93977	0.09098
R2	0.00821	0.98970	0.01614
R3	0.00711	0.99750	0.00291
A1, F1	0.03682	0.99649	0.10972
A2	0.01483	0.99697	0.01537
A3	0.00927	0.99163	0.01665
D1	0.01141	0.97594	0.07370
D2	0.01107	0.99719	0.00792
D3	0.00571	0.98920	0.00819
D4	0.00326	0.99968	7.84088×10^{-5}
	T = 320 °C		
Mechanism	$k(T)$ (min^{-1})	R^2	*RSS*
R1, F0	0.01353	0.94091	0.08643
R2	0.01411	0.99007	0.01504
R3	0.01220	0.99767	0.00262
A1, F1	0.06314	0.99636	0.10977
A2	0.02546	0.99714	0.01397
A3	0.01591	0.99195	0.01547
D1	0.01961	0.97657	0.06944
D2	0.01901	0.99736	0.00721
D3	0.00979	0.98890	0.00811
D4	0.00560	0.99965	8.31180×10^{-5}

Similar to the previous investigated pyrolysis process, in the case of beech wood pyrolysis (Table 3), the model-fitting method described by Eq. (2) also demonstrated the presence of several statistically equivalent reaction models with different values of k, at each of the considered operating temperatures (R3, D2 and D4 models at 280 °C, R3, D3 and D4 models at 290 °C, R3, F1, D3 and D4 models at 300 °C, R3, D2 and D4 models at 310 °C, R3, D2 and D4 models at 320 °C). The above presented results prevent us from determining with high reliability the exact analytical form of the function of the reaction mechanism, for both investigated pyrolysis processes.

It was found (from the Arrhenius equation) that almost the same value of the apparent activation energy and pre-exponential factor was obtained from all kinetic mechanisms, for both considered pyrolysis processes (E_a = 165.1 kJ mol^{-1} and $A = 3.869 \times 10^{12}$ min^{-1} (pine wood); E_a = 164.3 kJ mol^{-1} and $A = 4.958 \times 10^{12}$ min^{-1} (beech wood)). From these results, we can conclude the following: a) the kinetic data for both pyrolysis processes show a good fit to Eq. (2) regardless of the nature of the $g(\alpha)$ function assumed, and b) the apparent activation energy (E_a) obtained from the Arrhenius law is quite independent of the considered kinetic functions.

On the other hand, the above values of E_a for both investigated systems are different from the values of E_a calculated using the isoconversional analysis ($\langle E_a \rangle^{pine}$ = 139.3 kJ mol^{-1} and $\langle E_a \rangle^{beech}$ = 159.4 kJ mol^{-1}) (the difference between the values of E_a calculated by the Arrhenius equation and by the isoconversional analysis is less pronounced in the case of beech wood pyrolysis). From these results, it is very difficult to determine the reaction mechanism that can best describe the investigated pyrolysis processes and also to obtain the real values of the kinetic parameters (A and E_a). However, if a good global agreement in the entire reaction process is reached, one can expect a reasonable kinetic model.

Sharp *et al.*[29] have shown that reduced time scale plots facilitate the comparison of experimental data. The isokinetic data from a number of experimental runs should lie on a single curve. This curve can then be compared to that expected for any of a number of different theoretical rate equations (Table 1). The reduced time plots of $\alpha = \alpha(t/t_{0.50})$ for the pyrolysis process of pine wood at different operating temperatures are shown in Fig. 5.

It can be seen that the experimental data are not strictly isokinetic (the term *isokinetic* implies that at each operating temperature, all data points fall on the derived theoretical curve, which strictly corresponds to a single reaction model; i.e., there

is absolutely no deviation) for all of the considered operating temperatures (i.e., between 280 °C and 320 °C). These results show that the investigated pyrolysis process cannot be described by a *single rate equation* over the entire operating temperature range. However, we can see that the experiments at the lower operating temperatures (at 280 °C and 290 °C) lie on or between the theoretical reduced time plots, which correspond to D3 and D4 models (the diffusion controlled reactions). The models for D3 and D4 are very similar and because of this, they can hardly be distinguished below α = 0.60. The experiments at higher values of the operating temperatures (at 300, 310 and 320 °C) lie between a first-order reaction (F1) and diffusion controlled reactions (D1 and D2). In addition, we can assume that on increasing the operating temperature, the rate-determining step changes, and there is evidence that the investigated process could be multi-stage, or at least a mixture of two reaction mechanisms.

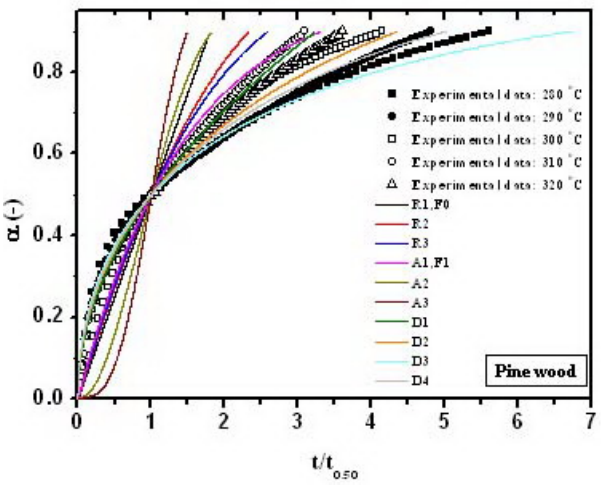

Figure 5: Reduced time plots ($t/t_{0.50}$) for the pyrolysis of pine wood at T = 280, 290, 300, 310 and 320 °C. The expected evolutions of the fraction transformed for the phase boundary (R1, F0, R2 and R3), nucleation (A1, F1, A2 and A3) and diffusion (D1, D2, D3 and D4) controlled reactions are shown by the colored lines. The experimental data for the pyrolysis process of pine wood are designated by symbols (Color reproduction in online version)

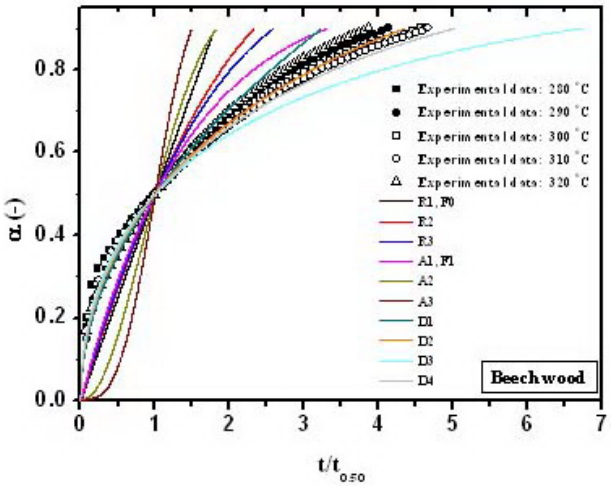

Figure 6: Reduced time plots ($t/t_{0.50}$) for the pyrolysis of beech wood at T = 280, 290, 300, 310 and 320 °C. The expected evolutions of the fraction transformed for the phase boundary (R1, F0, R2 and R3), nucleation (A1, F1, A2 and A3) and diffusion (D1, D2, D3 and D4) controlled reactions are shown by the colored lines. The experimental data for the pyrolysis process of beech wood are designated by symbols (Color reproduction in online version)

The reduced time plots of $\alpha = \alpha(t/t_{0.50})$ for the pyrolysis process of beech wood at different operating temperatures are shown in Fig. 6.

Also, for beech wood pyrolysis, the experimental data are not strictly isokinetic (*isokinetic* refers to the same as in the explanation given above for the pyrolysis of pine) at all of the considered operating temperatures (i.e., between 280 °C and 320 °C). However, unlike the data related to the pyrolysis of pine wood, in the present case, the experimental data are distributed only on or between the theoretical reduced time plots, which correspond to the diffusion group of reaction models (D1, D2, D3 and D4 models). Namely, at all of the considered operating temperatures, it is almost impossible to distinguish what diffusion models the experimental data belong to, especially at the lower values of α, to approximately α ≈ 0.55. After α ≈ 0.55, the experimental data show variability with the increase of operating temperature and of α value. All the experimental data, at the considered operating temperatures lie between D1 and D4 diffusion models. However, with an increase of α over the value of α = 0.65, the experimental data can then come closer to the theoretical reduced time plot which corresponds to the D4 diffusion model (Table 1).

Based on the above presented results, for both considered pyrolysis processes, we can conclude that it is impossible to distinguish between the kinetic models labeled A1, F1, D1, D2, D3 and D4, in agreement with the observations of Sharp *et al*.[29] If we observe carefully the results exposed

above, we could provisionally conclude that in the considered cases, the $t/t_{0.50}$ scale which was used is not sensitive enough, for discriminating among the A1, F1, D1, D2, D3 and D4 kinetic models. In this way, the discrimination among the models is difficult, because they are probably not statistically different.

Rather than fitting the data to one of a number of possible rate equations, and attempting to discern the rate controlling process by judging the quality of the fit between the data and each rate equation, it is possible to employ a general rate equation in which the function $f(\alpha)$ (Eq. (1)) is expressed in some general manner with a variable parameter that reflects the rate controlling mechanism. Such rate equations are sometimes called '*empirical rate equations*'. One such equation is commonly used and developed by Avrami.[28] The Avrami method expresses the general rate (Eq. (1)) in such a manner that the rate constant k and the controlling reaction mechanism (related to a parameter, m) can be determined simultaneously. The values of k and m can be calculated from the intercept and the gradient of an 'ln-ln' plot of the data ($\ln[-\ln(1-\alpha)] = m\ln k + m\ln t$). If a single reaction mechanism operates through the operating temperature range and several data sets are isokinetic, they will plot as a set of parallel lines with a constant value of m.

The data from the isothermal pyrolysis processes of pine and beech wood samples for a given conversion ranges ($\Delta\alpha$) (Table 4), at different operating temperatures (T = 280, 290, 300, 310 and 320 °C), are plotted as 'ln-ln' graphs in Fig. 7. Gradients (m) of the series of the lines presented in Fig. 7 are determined by the least-squares linear regression. The value of these gradients is characteristic of the rate-determining kinetic mechanism operating on that temperature.

From the least-squares linear regression analysis of these plots (Fig. 7), values for m and k have been obtained for both investigated systems, and they are given in Table 4.

From Table 4, we can see that for both pyrolysis processes, the isokinetic behavior of the runs at all of the considered operating temperatures was present. The isokinetic behavior is valid in a quite wide range of conversion values (Table 4). In the case of the applied 'ln-ln' graphs, the isokinetic behavior is directly related to the fact that gradient m does not change drastically its value, for example, from $m < 1$ to $m > 1$, which would then suggest a change in the rate-determining step (from diffusion controlled to phase-boundary controlled reactions), in the considered range of operating temperatures. In the case of pine wood pyrolysis, gradient m increases with operating temperature up to 300 °C. After T = 300 °C, gradient m slightly decreases to the value of m = 0.72. However, at all of the considered operating temperatures, the values of m are less than unity (i.e., the values are within the interval $0 < m < 1$). From these results, we can conclude that the pine wood pyrolysis process appears as isokinetic, in the wide range of the reaction extent, with a single dominant rate-limiting step. The average gradient, m, (Table 4) over the considered operating temperature range is 0.73. This value does not correspond to any one of the ten rate equations shown in Table 1. Rather, it is intermediate between the value expected for the first-order reaction and that expected for the diffusion control reaction.

However, upon a careful consideration of the value of m in pine wood pyrolysis (Table 4), we can see that the values of m at operating temperatures of 280 and 290 °C are more appropriate to the values of m, which correspond to the diffusion controlled process. At higher operating temperatures (300, 310 and 320 °C), the values of m are closer to the value characteristic of the first-order controlled process (F1, m = 1.00 (Table 1)). It seems likely, therefore, that the process is controlled by diffusion at lower operating temperatures, and then transferred to the regime, where it is controlled by the first-order reaction, at higher operating temperatures (Table 4). It can be pointed out that the above consideration of the results should be accepted with reserve, because the variation in the values of m (from m = 0.61 at 280 °C to m = 0.84 at 300 °C) may actually derive from the result of the experimental variation rather than a fundamental change in reaction mechanism. Therefore, it is necessary to carry out a more detailed kinetic analysis with an additional statistical analysis, which would enable us to unambiguously determine the reaction model, for the pyrolysis process of pine wood.

On the other hand, in the case of the beech wood pyrolysis, gradient m varies slightly with operating temperature, but unlike pine wood pyrolysis, gradient m does not exceed the value of m = 0.65 (Table 4). At all of the considered operating temperatures, the values of m are less than unity ($m < 1.00$), which directly corresponds to a process controlled by the diffusion

mechanism. The average gradient, *m*, (Table 4) over the considered operating temperature range is 0.60. This value is approximately located between the values of *m* in the cases of one- (D1) and two- (D2) dimensional diffusion mechanisms (Table 1). However, it is very difficult to differentiate between the different diffusion-controlled mechanisms (Table 1). Therefore, it is necessary to perform additional kinetic tests with the use of statistical methods for the purpose of unambiguous determination of the reaction model for the beech wood pyrolysis process.

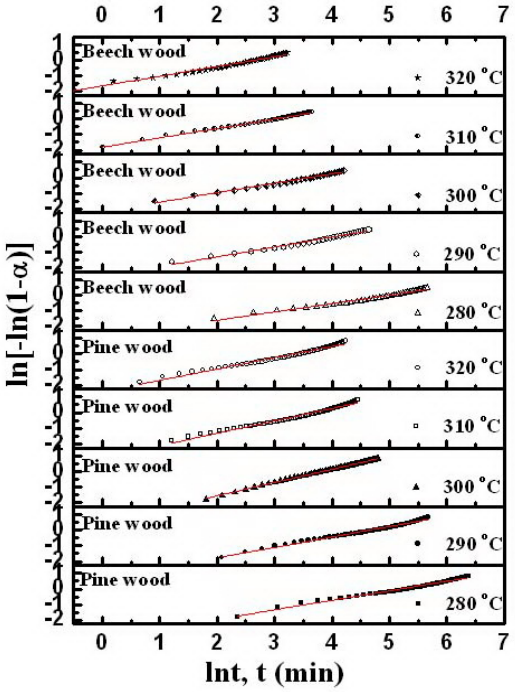

Figure 7: Avrami 'ln-ln' plots for the isothermal pyrolysis processes of pine and beech wood samples for given conversion fraction ranges (Δα) presented in Table 4, at different operating temperatures (*T* = 280, 290, 300, 310 and 320 °C); every plot is given in stack column panel (Color reproduction in online version)

Table 4
Values of rate constant (*k*) and gradient (*m*) for pine and beech wood pyrolysis at different operating temperatures, determined by the Avrami method

Pine wood				
Temperature, *T* (°C)	Conversion range, Δα	*k* (min^{-1}) (from intercept)	*m* (slope)	R^2 (Adj. R-Square)
280	0.16 - 0.90	0.00569	0.61 ± 0.01	0.98646
290	0.16 - 0.90	0.00964	0.67 ± 0.01	0.98605
300	0.15 - 0.90	0.01788	0.84 ± 0.01	0.99915
310	0.16 - 0.90	0.02582	0.79 ± 0.01	0.97759
320	0.15 - 0.90	0.04162	0.72 ± 0.01	0.97839
Average	-	0.02013	0.73 ± 0.01	-
Beech wood				
Temperature, *T* (°C)	Conversion range (Δα)	*k* (min^{-1}) (from intercept)	*m* (slope)	R^2 (Adj. R-Square)
280	0.20 - 0.80	0.00693	0.54 ± 0.01	0.97398
290	0.18 - 0.80	0.01695	0.63 ± 0.01	0.98257
300	0.20 - 0.80	0.02732	0.60 ± 0.01	0.98479
310	0.15 - 0.80	0.04879	0.60 ± 0.01	0.99217
320	0.17 - 0.80	0.07011	0.62 ± 0.02	0.97206
Average	-	0.03402	0.60 ± 0.01	-

In order to test the real quality of the linear fitting in Fig. 7, we have applied Tukey's test[39] to check the curvature of the residuals. Figs. 8 and 9 show the plots of residuals against the independent variable, for pine and beech wood pyrolysis processes, at different operating temperatures, respectively.

For both processes (Figs. 8 and 9), the graphs provide trend-free residual plots, in which the best fitting is clearly shown by the residual plot at 300 °C for pine wood pyrolysis, where it exhibits a nearly normal distribution of the residuals (Fig. 8). Consequently, the "favored" fitting is exactly at 300 °C for pine wood pyrolysis. On the other hand, it should be strictly noted that, in general, the tests for curvature points out that a high curvature indicates that the fit is very poor. The tests for curvature for our fitted results in Fig. 7 gave the following results: for pine – curvature = 0.22 (d[%] (deviation from the ideal prediction) = 0.41%) (280 °C), curvature = 0.30, (d[%] = 0.43%) (290 °C), curvature = 0.02 (d[%] = 0.03%) (300 °C), curvature = 0.50 (d[%] = 0.86%) (310 °C), curvature = 0.54 (d[%] = 0.89%) (320 °C), and for beech – curvature = 0.23 (d[%] = 0.48%) (280 °C), curvature = 0.15 (d[%] = 0.23%) (290 °C), curvature = 0.10 (d[%] = 0.17%) (300 °C), curvature = 0.08 (d[%] = 0.10%) (310 °C) and curvature = 0.33 (d[%] = 0.49%) (320 °C). These results suggest that we have low curvatures in both considered cases (the very high curvature values may go up to ± 70 or 80[39]). Therefore, the values of Adj. R-Square as R^2 = 0.97759 and R^2 = 0.97206 (Table 4) represent a very good fitting of the data by the direct application of the 'ln-ln' method. This reasoning applies to all other values of R^2 in Table 4.

Furthermore, for both considered pyrolysis processes, the rate constant k increases with an increase of the operating temperature (Table 4). (Globally, the increase in temperature accelerates the process, which is consistent with the general proposition of chemical kinetics). With the logarithmic form of the Arrhenius equation ($\ln k = \ln A - E_a/RT$), the values of k presented in Table 4 were used in order to determine the kinetic parameters, for pine and beech wood pyrolysis processes. From the Arrhenius plots (not shown) the following values of E_a and A were obtained: E_a = 135.6 ± 1.1 kJ mol^{-1} and $A = 3.694 \times 10^{10}$ min^{-1} (pine wood pyrolysis); E_a = 155.5 ± 1.5 kJ mol^{-1} and $A = 3.897 \times 10^{12}$ min^{-1} (beech wood pyrolysis). The obtained values of the apparent activation energy (E_a) using the Arrhenius plots for both investigated pyrolysis processes are in good agreement with the values of E_a calculated by the isoconversional method ($\langle E_a \rangle^{pine}$ = 139.3 kJ mol^{-1} and $\langle E_a \rangle^{beech}$ = 159.4 kJ mol^{-1}).

The time taken for a given conversion fraction (α) for pine and beech wood pyrolysis processes, can be estimated using the apparent activation energies and the pre-exponential factors, which have been shown above. The rate constants are derived from the Arrhenius equation for the operating temperature of interest, and the time taken for a given pyrolysis fraction to be obtained is calculated from the following form of the Avrami equation:

$$t = \frac{\exp\left\{m^{-1}\ln\left[-\ln(1-\alpha)\right]\right\}}{k} \quad (5)$$

The corresponding results using the values of E_a and A derived above and with m = 0.73 (pine wood) and m = 0.60 (beech wood) are presented in Table 5.

Based on the results shown in Table 5, there are differences in the values of t_{50} for a given extrapolated operating temperature range, in the case of the investigated pyrolysis processes. However, the difference in t_{50} values for each individual operating temperature is not enormously large, thus we should expect a similar transformation mechanism of the present reagents into pyrolysis products. In addition, in both cases, the increase in operating temperature, t_{50} is then significantly reduced, so that at high operating temperatures t_{50} reaches very small values.

The above established results should be used with caution, taking note of the limitations of extrapolating higher temperature kinetic data to the lower temperatures, and the possible dangers of inferring that the reaction mechanism is the same/almost the same throughout the operating temperature range. To remove any doubt about it, it is necessary to perform additional testing, including a more sophisticated approach, a combined kinetic and statistical analysis of the experimental data. In this case, it is necessary to find which of the observed kinetic models gives the lowest value of RSS (Residual sum of squares).[40] Meanwhile, the lowest value of RSS may not differ significantly from the second smallest. One is advised to use the F-test (Multiple hypothesis testing)[41] to check whether the difference in values of RSS is significant. Note that RSS can be readily converted to the variance, S^2, as:[40]

$$S^2 = \frac{RSS}{N - p} \quad (6)$$

where N is the total number of experimental points used in the calculation and p is the total number of kinetic parameters determined as a result of the calculation. The significance of the difference in two variances is readily checked by using the regular F-test.

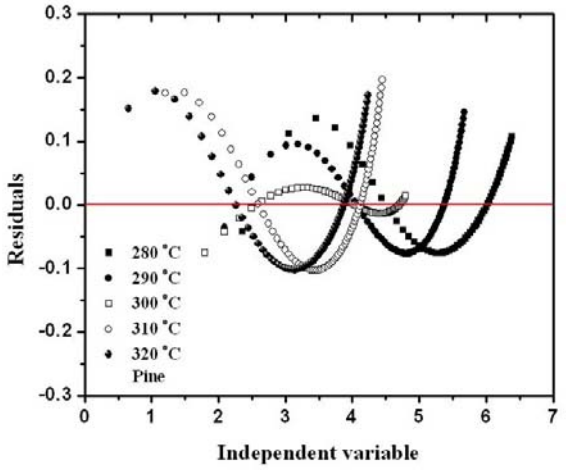

Figure 8: Residual plots of isothermal TG data for operating temperatures of T = 280, 290, 300, 310 and 320 °C, for pine wood pyrolysis (Color reproduction in online version)

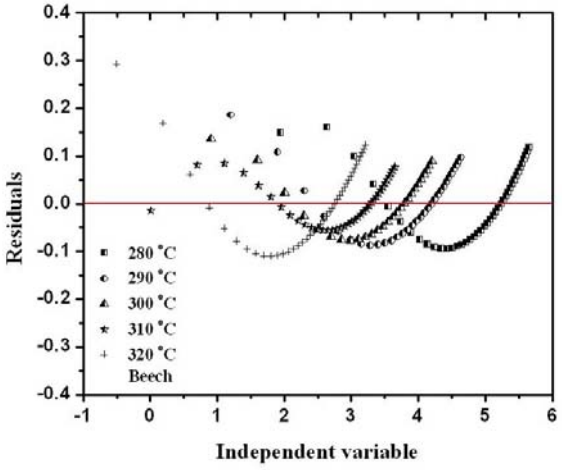

Figure 9: Residual plots of isothermal TG data for operating temperatures of T = 280, 290, 300, 310 and 320 °C, for beech wood pyrolysis (Color reproduction in online version)

Table 5
Time (t) values (in [min]) for transformation of 50% of solid pine and beech wood samples into pyrolysis products (half-life), in the extrapolating operating temperature range

Pine wood pyrolysis, 50% conversion							
T (°C)	240	250	260	340	360	380	400
t_{50} (min)	1041.60	567.36	316.16	5.84	2.52	1.15	0.55
Beech wood pyrolysis, 50% conversion							
T (°C)	240	250	260	340	360	380	400
t_{50} (min)	939.55	468.12	239.41	2.46	0.94	0.38	0.16

Table 6 shows RSS and S^2 values for diffusion group of reaction mechanisms (D1, D2, D3, D4) and the corresponding values of rate constants (k) calculated using Eq. (1), at different operating temperatures, for pyrolysis processes of the considered wood samples. Statistically, the most suitable kinetic models are marked with bold letters (Table 6).

We can see that based on the statistical analysis of the experimental data, the pyrolysis process of pine wood can be best described by the three-dimensional (D3) diffusion with spherical symmetry (Jander Eq.), at all of the considered operating temperatures (Table 6). In diffusion-controlled reactions, the rate of product formation decreases proportionally with the thickness of the product barrier layer. Namely, during the pyrolysis, the diffusion-controlled reactions mostly consist of the decomposition of large molecules of cellulose, hemicelluloses or lignin. In view of the D3 kinetic model, for globally describing the pyrolysis process of pine wood, it is important to say that the selected model should be taken into account as the diffusion of volatile products from the inside layers of the wood sample. Jander's model is used for diffusion-controlled solid-state reaction kinetics in a sphere. In this case, the diffusion of the pyrolysis

products arises from the degradation of three main components of the investigated wood sample (such as cellulose, hemicelluloses and lignin). Therefore, the diffusion in all three directions is important.

On the other hand, the most suitable kinetic model (from a statistical point of view) to describe the pyrolysis process of beech wood is the three-dimensional (D4) diffusion starting from the outside of a spherical particle (Ginstling-Brounstein Eq.) (valid for all of the considered operating temperatures (Table 6)). The general equations describe the diffusion-controlled reaction of a spherical particle of initial component to form a single concentric shell of the product by reaction with some other component. The reaction products are assumed to grow simultaneously as uniform and compact concentric shells with ideal contact at the interfaces as well as at the external surface of the sphere. Both elements are assumed to be mobile. The growth process is described in terms of chemical reactions and partitioning of the diffusion flux at phase boundaries.[42] Also, the above kinetic model should be viewed in the light of diffusion of volatile products (arising from the degradation processes of cellulose, hemicelluloses and lignin, respectively) from beech wood pyrolysis, with a slightly different geometry than in the case of the pine wood pyrolysis. Based on the presented results, D3 and D4 are the best reaction mechanisms to describe the pyrolysis processes of pine and beech wood samples, respectively. These mechanisms should be considered as one-step reaction mechanisms or global kinetic models for the mechanistic description of the complex pyrolysis processes.

Table 6
Values of *RSS* and S^2 for the diffusion group of reaction mechanisms (D1, D2, D3 and D4) and corresponding values of rate constants (k) calculated using Eq. (1), at different operating temperatures, for pine and beech wood pyrolysis

Mechanism	Pine wood				Beech wood			
	T (°C)	k (min^{-1})	*RSS*	S^2	T (°C)	k (min^{-1})	*RSS*	S^2
D1	280	0.00461	8.67776×10^{-6}	1.58×10^{-7}	280	0.00727	8.88409×10^{-5}	2.22×10^{-6}
D2		0.00221	1.05634×10^{-5}	1.92×10^{-7}		0.00348	9.38688×10^{-5}	2.35×10^{-6}
D3		5.15100×10^{-4}	6.61756×10^{-6}	$\mathbf{1.20 \times 10^{-7}}$		8.12792×10^{-4}	9.32899×10^{-5}	2.33×10^{-6}
D4		4.93590×10^{-4}	1.03179×10^{-5}	1.88×10^{-7}		7.77152×10^{-4}	8.82797×10^{-5}	$\mathbf{2.21 \times 10^{-6}}$
D1	290	0.00638	1.61027×10^{-5}	2.30×10^{-7}	290	0.01195	1.60317×10^{-4}	5.17×10^{-6}
D2		0.00306	1.95600×10^{-5}	2.79×10^{-7}		0.00578	1.68728×10^{-4}	5.44×10^{-6}
D3		7.12798×10^{-4}	1.60513×10^{-5}	$\mathbf{2.29 \times 10^{-7}}$		0.00133	1.67746×10^{-4}	5.41×10^{-6}
D4		6.83767×10^{-4}	1.90986×10^{-5}	2.73×10^{-7}		0.00129	1.89187×10^{-4}	$\mathbf{5.14 \times 10^{-6}}$
D1	300	0.00958	1.68803×10^{-4}	2.96×10^{-6}	300	0.02281	3.89658×10^{-4}	1.50×10^{-5}
D2		0.00467	1.46948×10^{-4}	2.58×10^{-6}		0.01099	3.83847×10^{-4}	1.48×10^{-5}
D3		0.00107	1.70190×10^{-5}	$\mathbf{2.99 \times 10^{-7}}$		0.00255	3.81034×10^{-4}	1.47×10^{-5}
D4		0.00104	1.49404×10^{-4}	2.62×10^{-6}		0.00245	3.56808×10^{-4}	$\mathbf{1.37 \times 10^{-5}}$
D1	310	0.01063	6.66781×10^{-5}	9.01×10^{-7}	310	0.03913	5.08170×10^{-4}	1.36×10^{-5}
D2		0.00512	7.75781×10^{-5}	1.05×10^{-6}		0.01905	5.85514×10^{-4}	1.58×10^{-5}
D3		0.00159	6.64456×10^{-5}	$\mathbf{8.98 \times 10^{-7}}$		0.00437	5.72634×10^{-4}	1.55×10^{-5}
D4		0.00119	7.61910×10^{-5}	1.03×10^{-6}		0.00425	4.94432×10^{-4}	$\mathbf{1.34 \times 10^{-5}}$
D1	320	0.01944	2.98184×10^{-4}	4.26×10^{-6}	320	0.04896	0.00751	1.88×10^{-4}
D2		0.00932	3.47338×10^{-4}	4.96×10^{-6}		0.02368	0.00774	1.94×10^{-4}
D3		0.00217	2.93862×10^{-4}	$\mathbf{4.20 \times 10^{-6}}$		0.00547	0.00772	1.90×10^{-4}
D4		0.00208	3.41218×10^{-4}	4.87×10^{-6}		0.00528	0.00748	$\mathbf{1.53 \times 10^{-4}}$

It should be noted that Agrawal[14] examined effective solid state mechanisms for the decomposition of not only wood samples, but also other lignocellulosic materials, and found that D3 and D4 mechanisms were effective mechanisms. Vlaev *et al.*[43] studied the decomposition of a lignocellulosic material, rice husk, and they found that the D4 mechanism is a Ginstling-Brounstein equation valid for the diffusion-controlled reactions starting on the exterior of spherical particles with uniform radius. In the literature, the F1(A1) mechanism was also adopted for the decomposition of lignocellulosic materials to describe the experimental data.[44] In the present study, the D3 and D4 diffusion mechanisms were found as effective mechanisms for the pyrolysis of the investigated wood samples, as compared to the F1(A1) mechanism.

In addition, it should be noted that the mechanisms involving a large set of parameters have also been proposed, based on the component decomposition rates.[9] The apparent activation energy of the global reaction presents largely variable values, roughly comprised between 89.0 and 175.0 kJ mol^{-1}. This can be the result of different heating conditions, different sample characteristics (size and wood variety) and of the mathematical treatment of the experimental data. In the present study, the obtained values of the apparent activation energies (E_a = 135.6 kJ mol^{-1} (pine wood pyrolysis) and E_a = 155.5 kJ mol^{-1} (beech wood pyrolysis)) lie within the above range of E_a values, for the global reaction mechanism of the wood pyrolysis process. On the other hand, the value of 135.6 kJ mol^{-1} for pine wood pyrolysis is in good agreement with the value of E_a (135.8 kJ mol^{-1}) obtained for the low operating temperature range (225-325 °C) of the waste wood (furniture - pine) pyrolysis.[45] The value of 155.5 kJ mol^{-1} obtained for beech wood is in good agreement with the values of E_a reported by Bruch *et al*.[46] (E_a = 149.5 kJ mol^{-1}) and by Branca *et al*.[47] (E_a = 148.6 kJ mol^{-1}).

The actual reaction scheme of wood pyrolysis is extremely complex because of the formation of over a hundred intermediate products. The pyrolysis of wood is, therefore, generally modelled on the basis of apparent kinetics. Ideally, the chemical kinetics model should account for primary decomposition reactions, as well as for secondary reactions. However, so far models have generally accounted for primary reactions through apparent kinetics and in some cases, some of the secondary reactions through multi-step reaction schemes.[48] In the light of the above presented results, some differences in the values of the kinetic parameters and diffusion geometry of the volatile products should be pointed out, probably resulting from sensitive alterations of the structure and the chemical composition of the investigated wood samples, taking place during pyrolysis. Namely, the lignin of softwoods is mainly built up from coniferyl- and *p*-coumaryl-alcohol, while in the case of hardwoods, the major components are coniferyl- and sinapyl-alcohol. The hemicellulose fraction of the hardwoods is mainly composed of glucuronxylans, which are thermally and hydrolytically more instable than glucomannans, which are dominant in the hemicelluloses of softwood.[49] Considering cellulose, there are no significant differences between the investigated wood samples (pine wood, cellulose (%wt) = 40, and beech wood, cellulose (%wt) = 45[50])) regarding structure and composition. However, the largest differences in the chemical composition of different wood species consist in the type and the content of extractives (pine wood, extractives (%wt) = 3.5, and beech wood, extractives (%wt) = 2.0[51])). A rather large value of E_a (135.6 kJ mol^{-1}) for pine wood may be attributed to the more thermally stable hemicelluloses, including the addition and the amount of extractives compared to hardwood (such as beech wood). The strong degradation of hemicelluloses through thermal decomposition of the wood sample has already been proven by several researchers.[51,52]

CONCLUSION

The pyrolysis process of pine and beech wood samples was investigated by the isothermal thermogravimetric technique, at five different operating temperatures (280, 290, 300, 310, and 320 °C), in a flowing stream of nitrogen gas. It was found that the isothermal pyrolysis of pine and beech wood samples can be described by the three-dimensional diffusion mechanisms, with different reaction geometry (Jander's type (D3) for pine, and Ginstling-Brounstein's type (D4) for beech wood). Tukey's test was applied in order to express the quality of the fit to the experimental data by applying the double logarithmic plots method. The estimated kinetic models for both pyrolysis processes represent the global one-step reaction mechanisms. Also, it was found that the obtained values of the apparent activation energies (E_a = 135.6 kJ mol^{-1} (pine wood) and E_a = 155.5 kJ mol^{-1} (beech wood)) lie within the range of E_a values, for the global reaction mechanism of the wood pyrolysis process (89.0-175.0 kJ mol^{-1}). In addition, some differences were established in the values of the kinetic parameters (E_a, A) and diffusion geometry of the volatile products, probably resulting from sensitive alterations of the structure and the chemical composition of the investigated wood samples, occurring during the investigated pyrolysis processes.

ACKNOWLEDGEMENTS: The authors would like to thank the Ministry of Science and Environmental Protection of Serbia (Projects 172015 and III43009).

REFERENCES

[1] A. Demirbas, G. Arin, *Energ. Sources*, **24**, 471 (2002).
[2] B. V. Babu, A. S. Chaurasia, *Energ. Convers. Manag.*, **44**, 2135 (2003).
[3] B. V. Babu, A. S. Chaurasia, *Energ. Convers. Manag.*, **44**(**14**), 2251 (2003).
[4] B. V. Babu, A. S. Chaurasia, *Energ. Convers. Manag.*, **45**(**1**) 53 (2004).
[5] B. V. Babu, A. S. Chaurasia, *Chem. Eng. Sci.*, **59**, 611 (2004).
[6] M. Dietenberger, *Procs. 39th Annual Conference*, North American Thermal Analysis Society, August 7-10, 2001, Des Moines, Iowa, USA, pp. 1-12.
[7] D. F. Arseneau, *Can. J. Chem.*, **39**, 1915 (1961).
[8] F. Thurner, U. Mann, *Ind. Eng. Chem. Process Des. Dev.*, **20**, 482 (1981).
[9] C. A. Koufopanos, G. Maschio, A. Lucchesi, *Can. J. Chem. Eng.*, **67**, 75 (1989).
[10] C. A. Koufopanos, N. Papayannanos, G. Maschio, A. Lucchesi, *Can. J. Chem. Eng.*, **69**, 907 (1991).
[11] A. K. Sadhukhan, P. Gupta, R. K. Saha, *Bioresource Technol.*, **100**, 3134 (2009).
[12] Y. Kumagai, T. Ohuchi, *Mokuzai Gakkaishi*, **6**, 265 (1973).
[13] T. Hirata, H. Abe, *Mokuzai Gakkaishi*, **9**, 451 (1973).
[14] R. K. Agrawal, *Thermochim. Acta*, **91**, 343 (1985).
[15] F. Bonnefoy, P. Gilot, G. Prado, *J. Anal. Appl. Pyrol.*, **25**, 387 (1993).
[16] B. M. Wagenaar, W. Prins, W. P. M. Van Swaaij, *Fuel Process. Tech.*, **36**, 291 (1993).
[17] A. Raimo, E. Kuoppala, P. Oesch, *J. Anal. Appl. Pyrol.*, **36**, 137 (1996).
[18] M. Nik-Azar, M. R. Hajaligol, M. Sohrabi, B. Dabir, *Fuel Process. Tech.*, **51**, 7 (1997).
[19] C. Di Blasi, C. Branca, *Ind. Eng. Chem. Res.*, **40**, 5547 (2001).
[20] M. Müller-Hagedorn, H. Bockhorn, L. Krebs, U. Müller, *J. Anal. Appl. Pyrol.*, **68-69**, 231 (2003).
[21] T. Willner, G. Brunner, *Chem. Eng. Tech.*, **28**, 1212 (2005).
[22] E. Grieco, G. Baldi, *Chem. Eng. Sci.*, **66**, 650 (2011).
[23] M. Y. L. Chew, N. Q. An Hoang, L. Shi, *Int. J. Archit. Sci.*, **8**, 17 (2011).
[24] L. Yang, X. Chen, X. Zhou, W. Fan, *Combust. Flame*, **133**, 407 (2003).
[25] V. Hankalin, T. Ahonen, R. Raiko, *Procs. Finnish-Swedish Flame Days*, January 28-29, 2009, Naantali, Finland, pp. 1-16.
[26] A. K. Galwey, M. E. Brown, "Thermal Decomposition of Ionic Solids", Elsevier, Amsterdam, The Netherlands, first ed., 1999, pp. 75-110.
[27] S. Vyazovkin, *Thermochim. Acta*, **355**, 155 (2000).
[28] M. Avrami, *J. Chem. Phys.*, **7**, 1103 (1939).
[29] J. H. Sharp, G. W. Brindley, A. B. N. Narahari, *J. Am. Ceram. Soc.*, **49**, 379 (1966).
[30] J. D. Hancock, J. H. Sharp, *J. Am. Ceram. Soc.*, **55**, 74 (1972).
[31] K. S. Go, S. R. Son, S. D. Kim, *Int. J. Hydrogen Energ.*, **33**, 5986 (2008).
[32] R. Gupta, D. N. D. Mittal, *Int. J. Eng. Sci. Tech.*, **2**, 5088 (2010).
[33] D. K. Shen, S. Gu, J. Baosheng, M. X. Fang, *Bioresource Technol.*, **102**, 2047 (2011).
[34] F. C. Beall, *Wood Fiber*, **1**, 215 (1969).
[35] F. Shafizadeh, in "The Chemistry of Solid Wood", edited by R. M. Rowell, Advances in Chemistry Series 207, American Chemical Society, Washington, DC, 1984, pp. 489-530.
[36] P. T. Williams, S. Besler, *Renew. Energ.*, **7**, 233 (1966).
[37] M. Bajus, *Petroleum and Coal*, **52**, 207 (2010).
[38] F. Aarsen, C. Beenackers, V. Swaaij, in "Fundamentals of Thermochemical Biomass Conversion", edited by R. P. Overend, T. A. Milne, L. K. Mudge, Elsevier Applied Science Publishers, London, UK, 1985, pp. 691-715.
[39] R. D. Cook, S. Weisberg, "Applied Regression Including Computing and Graphics", Hoboken, NJ, John Wiley and Sons, USA, 1999, pp. 85-99.
[40] S. Vyazovkin, A. K. Burnham, J. M. Criado, L. A. Pérez-Maqueda, C. Popescu *et al.*, *Thermochim. Acta*, **520**, 1 (2011).
[41] J. E. Freund, B. M. Perles, "Modern Elementary Statistics", 12th edition, Pearson Prentice Hall, Upper Saddle River, New York, 2006, pp. 85-98.
[42] J. R. Frade, M. Cable, *J. Am. Ceram. Soc.*, **75**, 1949 (1992).
[43] L. T. Vlaev, I. G. Markovska, L. A. Lyubchev, *Thermochim. Acta*, **406**, 1 (2003).
[44] S. S. Abdullah, S. Yusup, M. M. Ahmad, A. Ramli, L. Ismail, *Int. J. Chem. Biol. Eng.*, **3**, 137 (2012).
[45] J. Reina, E. Velo, L. Puigjaner, *Ind. Eng. Chem. Res.*, **37**, 4290 (1998).
[46] C. Bruch, B. Peters, T. Nussbaumer, *Fuel*, **82**, 729 (2003).
[47] C. Branca, A. Albano, C. Di Blasi, *Thermochim. Acta*, **429**, 133 (2005).
[48] C. Di Blasi, *Progress Energ. Comb. Sci.*, **34**, 47 (2008).
[49] K. Németh, "Faanyagkémia – Kémiai szerkezet, reakciók. Mezõgazdasági Szaktudás Kiadó", Budapest, Hungary, 1997, pp. 19-27.
[50] A. Pfriem, PhD Dissertation, TU Dresden, Germany, 2006, pp. 87-106.
[51] M. S. Sweet, J. E. Winandy, *Holzforschung*, **53**, 311 (1999).
[52] J. E. Winandy, P. K. Lebow, *Wood Fiber Sci.*, **33**, 239 (2001).